Modeling and Validation of Cardiovascular System with Rotary Left Ventricular Assist Device

Meena Priya C[1] and Arun Kumar Srirangan[2]*
[1]Department of EIE, Kumaraguru college of Technology, Saravanampatti, Coimbatore-641049
[2]School of Mechanical Engineering, SASTRA University, Thanjavur, Tamilnadu-613401
***Corresponding author: E-Mail: arun1988@gmail.com: Tel: +91-9943989906**

ABSTRACT

Heart disease is one among the major causes for the prevalent death rate in this world. Heart transplantation is the common therapy carried out for heart failures in earlier days. However recently, the Ventricular Assist Devices (VADs) emerged as an alternative therapy for congestive heart failures due to the shortage of donor hearts. In this paper, model of the cardiovascular system was referred and developed which simulated the hemodynamics of the natural heart. This simulated hemodynamics must comply with the waveforms of the natural heart's cardiac cycle available in the benchmarks. The rotary Left VAD (LVAD) was also modeled and combined with the cardiovascular model to simulate the diseased heart with LVAD parameters. Thus the mathematical modeling of the combined cardiovascular system and LVAD were simulated and a comparative analysis was done.

KEY WORDS: Cardiovascular System, Vad, Rotary Lvad, Cardiac Cycle.

1. INTRODUCTION

One of the best therapies for end stage congestive heart failure is heart transplantation. However, the unavailability of heart donors makes it difficult to proceed with the treatment. An evolving alternate option for this problem is the usage of VADs (Ohlsson, 1998). The VADs are mechanical devices which assist a native weak heart in its pumping action (Simaan, 2009) by regulating the Cardiac Output (CO) and the Mean Arterial Pressure (MAP) (Da Xu, 2009). The LVADs are special category of VADs which assists the left ventricle of the heart to pump blood to the other body parts (Poirier, 1997). This acts as a bridge between the left ventricle and aorta. It is used either as a destination therapy or bridge to transplant (Frazier, 1999).

2. MATHEMATICAL MODELING

The cardiovascular system and the LVAD were first modeled into a lumped parameter electrical circuit model and then using laws from circuit theory, it was translated into a set of differential equations (Ferreira, 2005; Faragallah, 2011).

Assumptions: The complex dynamic cardiovascular system was difficult to model mathematically. Since the model of this system was to be used in conjunction with the LVAD, during the development of electrical circuits, only the left side of the heart with the systemic circulation was considered. It was assumed that the right heart and the pulmonary circulations were healthy and working as expected. Also their effects on the LVAD system were considered negligible.

Table.1. Electrical analogue of the cardiovascular system

Cardiovascular system	Electrical system
Blood flow	Current
Compliance	Capacitance
Inertance	Inductance

Cardiovascular System:

Electrical analogue of the system: The lumped parameter circuit model of the cardiovascular system was developed with reference to the electrical analogue of the system as tabulated in the Table.I. The relationship between the blood flow (Q), pressure difference (ΔP) and the blood vessel resistance (R_{vasc}) was represented similar to the Ohm's law as given below,

$$Q = \frac{\Delta P}{R_{vasc}} \quad (1)$$

$$I = \frac{V}{R} \quad (2)$$

Compliance is a measure of the ability of the blood vessel wall to expand and contract in response to the changes in the pressure. This can be defined as the ratio of the change in volume (ΔVol) to the change in pressure (ΔP). The capacitor was used to model the vascular compliance since it describes how much charge (Δq) can be stored on a capacitor for a given change in voltage (Δv)

$$C_{vasc} = \frac{\Delta Vol}{\Delta P} \quad (3)$$

$$C = \frac{\Delta q}{\Delta v} \quad (4)$$

The blood inertance (L_{vasc}) relates the pressure drop with the rate of change of flow. This was modeled using the concept of inductance (L) in electric circuits.

$$P(t) = L_{vasc}\frac{dQ(t)}{dt} \quad (5)$$

$$v(t) = L\frac{di(t)}{dt} \quad (6)$$

Electrical circuit of the system: The mathematical model of the system needs to be ensured that the output of the device reflects the oscillatory nature of the healthy heart for an extended duration of time. The simulated waveforms should be similar to the waveforms of the natural heart's cardiac cycle (Simaan, 2009; Stergiopulos, 1996; Ferreira, 2005). The lumped parameter electric circuit model (Simaan, 2009; Faragallah, 2011) for the cardiovascular system where each block was characterised by its own resistance, compliance, pressure and volume of blood is represented in Figure.1.

Here the preload and the pulmonary circulations of the heart were represented by the capacitance (C_R). The afterload was represented by the four elements Windkessel model (Stergiopulos, 1996) containing R_C, L_S, C_S and R_S. The model parameter values (Kowar, 2011; Choung, 1998) considered for the electrical circuit are tabulated in Table II. The value of R_S were varied to simulate different levels of activities of the body. Small values of R_S were used to simulate high levels of activity such as walking or running. High values of SVR were used to simulate low level of activity such as rest or sleeping. In this model, a value of R_S = 1.0 mmHg.s/ml was used to denote normal level of activity (Simaan, 2009).

Table.2. Model parameter values of the electrical circuit

Parameters	Physiological Meaning	Value
Resistances (mmHg.s/ml)		
R_S	Systemic Vascular Resistance (SVR)	1.0000
R_M	Mitral Valve Resistance	0.0050
R_A	Aortic Valve Resistance	0.0010
R_C	Characteristic Resistance	0.0398
Compliances (ml/mmHg)		
C(t)	Left Ventricular Compliance	Time Varying
C_R	Left Atrial Compliance	4.4000
C_S	Systemic Compliance	1.3300
C_A	Aortic Compliance	0.0800
Inertances (mmHg.s^2/ml)		
L_S	Inertance of blood in Aorta	0.0005
Valves		
D_M	Mitral Valve	-
D_A	Aortic Valve	-

Table.3. Cardiac cycle phase and diode states

Modes	Diode circuit states		Phases
	D_M	D_A	
1	Open	Open	Isovolumic Relaxation
2	Short	Open	Filling
1	Open	Open	Isovolumic Contraction
3	Open	Short	Ejection
-	Short	Short	Not feasible

Table4. State variables

Variable	Physiological meaning
$x_1(t)$	Left Ventricular Pressure
$x_2(t)$	Left Atrial Pressure
$x_3(t)$	Arterial Pressure
$x_4(t)$	Aortic Pressure
$x_5(t)$	Total Flow

Also, the compliance of the system was represented in terms of elastance by the Eq. (7). The mathematical representation of the elastance and the normalized elastance in terms of the double hill function (Ferreira, 2005; Faragallah, 2011) can be given as follows in equations (8) and (9) respectively.

$$C(t) = \frac{1}{E(t)} \quad (7)$$

$$E(t) = (E_{max} - E_{min}) * E_n(t_n) + E_{min} \quad (8)$$

$$E_n(t_n) = 1.55*\left[\frac{\left(\frac{t_n}{0.7}\right)^{1.9}}{1+\left(\frac{t_n}{0.7}\right)^{1.9}}\right]*\left[\frac{1}{1+\left(\frac{t_n}{1.17}\right)^{21.9}}\right] \quad (9)$$

$$t_n = t / T_{max} \quad (10)$$

$$T_{max} = 0.2 + 0.15 * t_c \quad (11)$$

$$t_c = 60 / HR \quad (12)$$

Here, E_{max} gives the End Systolic Pressure Volume Relationship (ESPVR), E_{min} gives the End Diastolic Pressure Volume Relationship (EDPVR), t_c represents one cardiac cycle interval and HR is the heart rate considered. The electrical circuit includes two ideal diodes for mitral and aortic valves. If the diode was short circuit, it simulated the open state of the valve and for closed state of the valve; the diode was made as open circuit. The different phases of the cardiac cycle with respect to the diode states and state variables considered are tabulated in Table.3, (Simaan, 2009; Simaan, 2009) and IV respectively. However by appropriately modeling the diode as nonlinear elements, all the phases can be represented by a single differential equation.

State space representation: The state space representation of the cardiovascular system (Simaan, 2009; Simaan, 2009; Faragallah, 2011) can be given as,

$$\dot{x}(t) = A_C(t)\, x(t) + B_c(t)\, p(t) \quad (13)$$

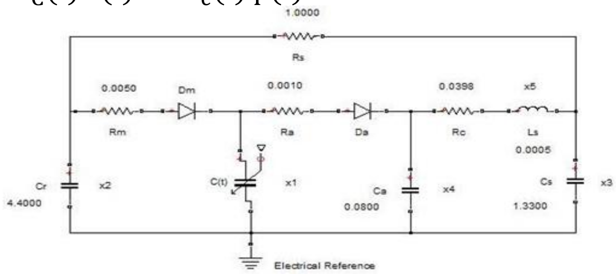

Figure.1. Electrical circuit of the cardiovascular system

$$A_c(t) = \begin{bmatrix} -\frac{C'(t)}{C(t)} & 0 & 0 & 0 & 0 \\ 0 & -\frac{1}{R_S C_R} & \frac{1}{R_S C_R} & 0 & 0 \\ 0 & \frac{1}{R_S C_S} & -\frac{1}{R_S C_S} & 0 & \frac{1}{C_S} \\ 0 & 0 & 0 & 0 & -\frac{1}{C_A} \\ 0 & 0 & -\frac{1}{L_S} & \frac{1}{L_S} & -\frac{R_C}{L_S} \end{bmatrix} \quad (14)$$

$$B_c(t) = \begin{bmatrix} \frac{1}{C(t)} & -\frac{1}{C(t)} \\ -\frac{1}{C_R} & 0 \\ 0 & 0 \\ 0 & \frac{1}{C_A} \\ 0 & 0 \end{bmatrix} \quad (15)$$

$$p(t) = \begin{bmatrix} \frac{1}{R_M} r(x_2 - x_1) \\ \frac{1}{R_A} r(x_1 - x_4) \end{bmatrix} \qquad r(x) = \begin{cases} x, & if\ x \geq 0 \\ 0, & if\ x < 0 \end{cases} \quad (16)$$

Here $A_c(t)$ and $B_c(t)$ are state space matrices of order 5×5 and 5×2 respectively. The nonlinear behavior of the diodes was represented by the ramp function r(x). This allowed the model to simulate the four phases of the cardiac cycle. In the contraction and relaxation phases, x_1 (t) > x_2 (t) and $x_4(t) > x_1(t)$. Hence the two ramp functions in the model $r(x_2 - x_1)$ and $r(x_1 - x_4)$ were equal to zero by making D_M and D_A open circuit respectively.

Also in the filling phase, x_4(t) < x_1 (t) and this lead the ramp function $r(x_1 - x_4)$ to have a value equal to the voltage difference across the diode D_M and its resistance R_M. Similarly in the ejection phase, x_1 (t) < x_2 (t) and the ramp function $r(x_2 - x_1)$ had a value equal to the voltage difference across the diode D_A and its resistance R_A.

Table.5. Model parameters of the LVAD pump

Parameters	Physiological Meaning	Value
Resistances (mmHg.s/ml)		
R_i	Inlet resistance of cannulae	0.0677
R_p	Pump resistance	0.17070
R_0	Outlet resistance of cannulae	0.0677
Inertances (mmHg.s^2/ml)		
L_i	Inlet inertance of cannulae	0.0127
L_p	Pump inertance	0.02177
L_0	Outlet inertance of cannulae	0.0127
Constants (mmHg/rpm^2)		
β	Pump dependent constant	$9.9025 * 10^{-7}$

LVAD model: The LVAD pump considered was a second generation axial flow rotary blood pump that was driven by a DC motor (Poirier, 1997; Frazier, 1999). The LVAD pump model need to be developed from its electrical equivalent. The electrical circuit representation of the pump is represented in the Figure.2. The rotation of the impeller of the pump causes a high pressure difference that can be expressed as the sum of the pressure differences across the inlet cannulae (H_i), the pump (H_p) and the outlet cannulae (H_o).

$$LVP(t) - AoP(t) = H_i + H_p + H_o \quad (17)$$

$$H_i = R_i Q_p(t) + L_i \frac{dQ_p(t)}{dt} \quad (18)$$

$$H_p = R_p Q_p(t) + L_p \frac{dQ_p(t)}{dt} - \beta\omega^2(t) \quad (19)$$

$$H_0 = R_0 Q_p(t) + L_0 \frac{dQ_p(t)}{dt} \quad (20)$$

Here ω(t) is the rotational speed of the pump. The model parameters of the electrical circuit are tabulated in the Table V. The rearranged form of Eq. (17) was given by Eq. (21) which was formulated by using the equations (18), (19), (20).

$$LVP(t) - AoP(t) = R^* Q_p(t) - L^* \frac{dQ_p(t)}{dt} - \beta\omega^2(t) \quad (21)$$

$$R^* = R_i + R_o + R_p + R_{su} \quad (22)$$

$$L^* = L_i + L_o + L_p \quad (23)$$

The parameter which affected the LVAD model was the rotational speed of the pump. However in reality, the pump was controlled by the motor current which in turn controls the motor speed. Thus the model was reformulated in such a way as to introduce pump motor current instead of pump speed as the independent control variable. The pressure gain across the pump (H_p) was modeled using the relation between the electrical power supplied to the pump motor (P_e) and the hydrodynamic power generated by the pump (P_p) which was scaled by the pump efficiency (η) (Faragallah, 2011)

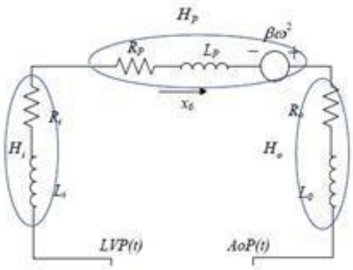

Figure.2. Electrical equivalent of LVAD pump

$$P_p = \eta P_e \quad (24)$$

$$P_e = V * i(t) \quad (25)$$

$$P_p = \rho g H_p Q \quad (26)$$

Rearranging the above equations for pressure gain and comparing it with the relationship of pump speed generalizes the above Eq. (22) in terms of pump flow (Q). The model parameters of the current based model of LVAD pump (Faragallah, 2011) is tabulated in Table VI.

$$\rho g H_p Q = \eta V i(t) \quad (27)$$

$$H_p = \frac{\eta V}{\rho g} . \frac{i(t)}{Q} \quad (28)$$

$$H_p = \gamma \frac{i(t)}{Q} \quad (29)$$

$$H_p = \beta\omega^2(t) \quad (30)$$

$$\omega(t) = \sqrt{\frac{\gamma\, i(t)}{\beta\, Q(t)}} \quad (31)$$

Table.6. Model Parameters of the current based LVAD

Parameters	Value	Physiological meaning
ρ	13,600	Density of the reference fluid (kg/m3)
g	9.8	Acceleration of gravity (m/s2)
η	100%	Pump efficiency

$$LVP(t) - AoP(t) = R^* Q_p(t) - L^* \frac{dQ_p(t)}{dt} - \frac{\gamma\, i(t)}{Q(t)} \quad (32)$$

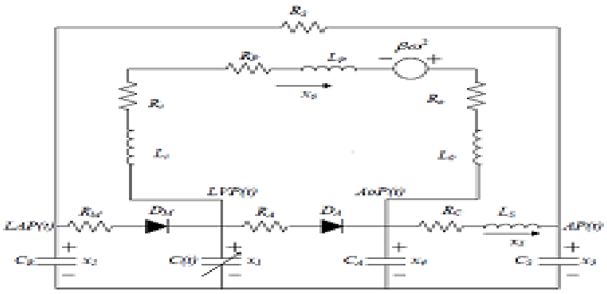

Figure.3. Electrical equivalent of combined model

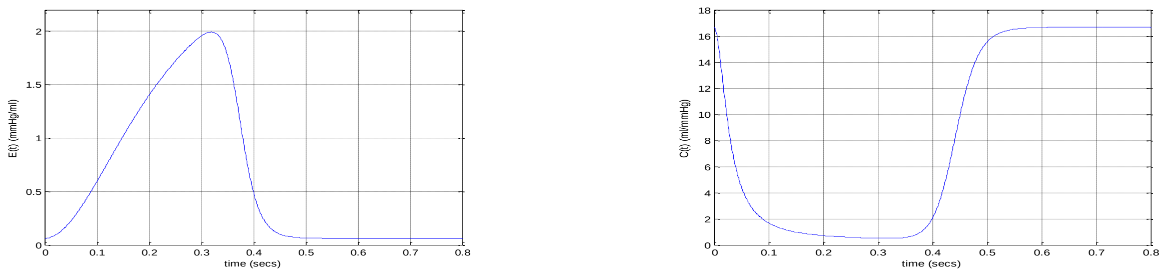

Figure.4(a) Elastance function **(b) Compliance function**

Combined system: A combined model of LVAD and cardiovascular system was derived by adding the first order model of LVAD to the fifth order model of cardiovascular system. The electrical equivalent of the combined model is depicted in the following Figure.3. The sixth state variable equation of the combined model was derived by rearranging the Eq. (32). The state space representation of the combined model gave the sixth order mathematical model that represented the interaction between the cardiovascular system and the LVAD. Thus a nonlinear time varying model that was controlled by increasing or decreasing the pump motor current i(t) was derived.

$$\dot{x_6}\,(t) = \frac{1}{L^*}\,x_1(t) - \frac{1}{L^*}\,x_4(t) - \frac{R^*}{L^*}\,x_6(t) + \frac{\gamma}{L^* x_6}\,i(t) \quad (33)$$

$$\dot{x}(\mathrm{t}) = \mathrm{A_C(t)x(t)} + \mathrm{B_c(t)p(t)} + \mathrm{b\,u(t)} \quad (34)$$

$$A_c(t) = \begin{bmatrix} -\frac{C'(t)}{C(t)} & 0 & 0 & 0 & 0 & \frac{-1}{C(t)} \\ 0 & -\frac{1}{R_S C_R} & \frac{1}{R_S C_R} & 0 & 0 & 0 \\ 0 & \frac{1}{R_S C_S} & -\frac{1}{R_S C_S} & 0 & \frac{1}{C_S} & 0 \\ 0 & 0 & 0 & 0 & -\frac{1}{C_A} & \frac{1}{C_A} \\ 0 & 0 & -\frac{1}{L_S} & \frac{1}{L_S} & -\frac{R_C}{L_S} & 0 \\ \frac{1}{L^*} & 0 & 0 & \frac{-1}{L^*} & 0 & \frac{-R^*}{L^*} \end{bmatrix} \quad (35)$$

$$B_c(t) = \begin{bmatrix} \frac{1}{C(t)} & -\frac{1}{C(t)} \\ -\frac{1}{C_R} & 0 \\ 0 & 0 \\ 0 & \frac{1}{C_A} \\ 0 & 0 \\ 0 & 0 \end{bmatrix} \qquad b = \begin{bmatrix} 0 \\ 0 \\ 0 \\ 0 \\ 0 \\ \frac{\gamma}{L^* x_6} \end{bmatrix} \quad (36)$$

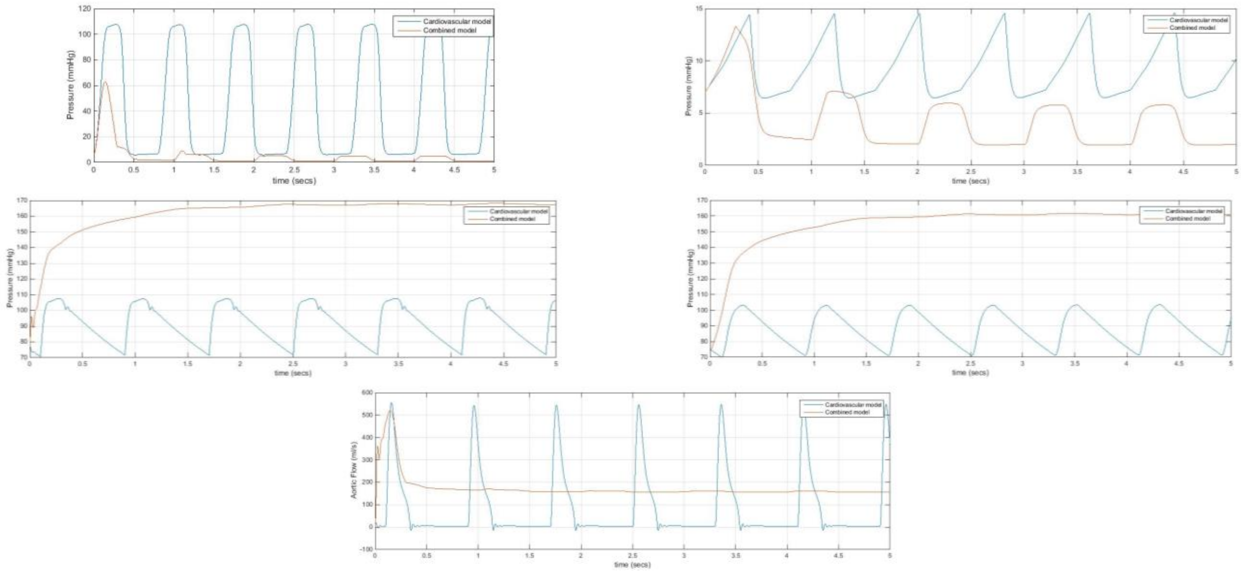

Figure.5. Hemodynamics of Cardiovascular system

3. SIMULATION RESULTS

The solution of the autonomous cardiovascular system was oscillatory due to the cyclic nature of the elastance, compliance and the state space element A_{11}. The elastance function over one cardiac cycle by taking the values of healthy heart $E_{max,}$ E_{min} and HR – 2, 0.06 mmHg/ml 75 bpm as shown in Figure.4.

The simulated waveforms of the cardiovascular system complied with the standard hemodynamic variables over the cardiac cycle (Simaan, 2009; Simaan, 2009). The LVAD pump used in this model was a second generation axial flow pump which generated changes in the hemodynamic conditions of the patients. The changes in the simulated waveforms of the cardiovascular hemodynamics after combining with LVAD pump are depicted in Figure.5.

In the elastance function, till 0.4 secs systolic phase occurred, this was eventually followed by the diastolic phase. The elastance is inversely proportional to the volume which increased during systolic and decreased during the diastolic phase. However the compliance function decreased during systolic phase since the volume of the ventricle was ejected out to the arteries. The compliance function increased in the diastolic phase since the ventricle was filled with blood from the systemic and pulmonary circulations. The A_{11} state space element was simulated using elastic function and its cyclic nature was verified.

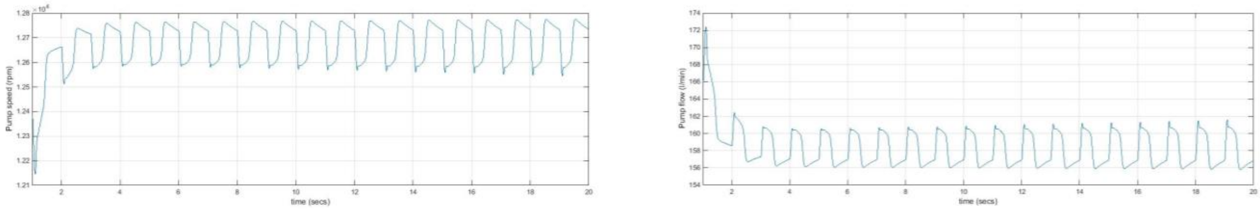

Figure.6. Dynamics of LVAD pump speed and flow

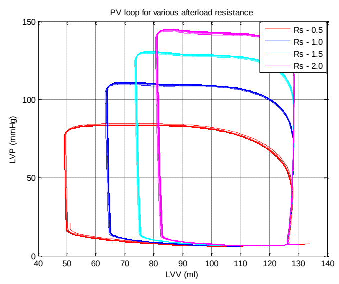

Figure.7(a) PV loop for afterload

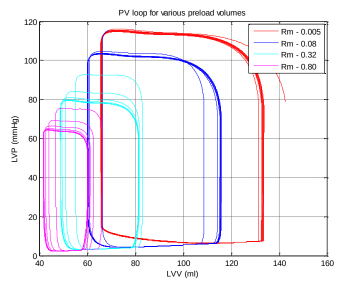

(b) PV loop for various preload

In the hemodynamics of the cardiovascular system, the aortic flow waveform was validated by analyzing the LVP and AoP at that particular instant. The blood flow through aorta occured only when the left ventricular pressure exceeded the aortic pressure. When the LVP decreases below AoP the aortic valve closes hence there will not be any flow of blood through the aorta. Also the LVAD parameters of pump flow and pump speed were analyzed by a constant pump motor current input. The signature of the simulated LVAD parameters was depicted in Figure.6.

Model Validation: The simulated cardiovascular system should be validated such that it was working as expected by varying either the preload or the afterload values (Simaan, 2009). The preload was varied by varying the systemic vascular resistance (R_S) and the resultant PV loop is depicted in the figure.7 (a). The afterload was varied by varying the mitral valve resistance (R_M) and the resultant PV loops are depicted in the figure.7 (b).

In the Pressure Volume loops of afterload, the value of R_s can be correlated to the physical activity of the person (Suga, 1974). Small values of R_s were used to simulate high level of physical activity. During high level of physical activity more amount of blood was be pumped out of the ventricle to match the higher oxygen saturation level. Hence the pressure level of the heart decreased. Similarly for low level of physical activity, large values of R_s were used. For low level of physical activity, comparatively less amount of blood was ejected from the ventricle since there was only less requirement of oxygen. Hence the pressure was very high for this case.

Similarly in the PV loops of preload, the values of mitral valve resistance are used to vary the preload volume of the system (Suga, 1974). The lower the resistance of the mitral valve, the higher was the volume of the blood filled inside the ventricle. Hence the pressure also increased correspondingly for lower values of mitral valve resistance. Similarly for the higher values of mitral valve, the resistance offered to the filling of ventricle was comparatively higher. Hence the ventricular volume was lower and correspondingly the pressure values were also comparatively less for this case.

4. CONCLUSION

Thus a combined mathematical model was developed which simulated the hemodynamics of the heart and the LVAD parameters. This was used to estimate and study the cardiovascular parameters that were difficult to measure in practical in-vivo compatibility tests. The combined model is regarded as a bio-mechanical coupled system where the dynamics of the heart and the pump are interconnected influencing each other.

REFERENCES

Choung Y, Boston J.R, Simaan M.A, Antaki J.F, Estimation of Systemic Vascular Bed Parameters for Artificial Heart Control, IEEE Transactions on Automatic Control, 43, 1998, 765-778.

Da Xu, Olivier B and Mukkamala R, Cardiac Output and Left Atrial Pressure Monitoring by Right Ventricular Pressure Waveform Analysis for Potential Implantable Device Application, IEEE Transactions on Biomedical Engineering, 56, 2009, 2335 – 2339.

Faragallah G, Wang Y, Divo E and Simaan M.A, A new control system for left ventricular assist devices based on patient-specific physiological demand, in Proc. Int. Conf. on Inverse Problems in Eng., Orlando, FL, 2011.

Faragallah G, Wang Y, Divo E and Simaan M.A, A new current-based control model of the combined cardiovascular and rotary left ventricular assist device, in Proc. Amer. Contr. Conf., San Francisco, CA, 2011.

Ferreira A, Chen S, Simaan M.A, Boston J.R, Antaki J.F, A Nonlinear State-space Model of a Combined Cardiovascular System and a Rotary Pump, Proceedings of the 44th IEEE Conference on Decision and Control, 2005, 897 – 902.

Frazier H and Myers T.J, Left ventricular assist systems as a bridge to myocardial recovery, Annals Thoracic Surg., 68, 1999, 734–741.

Kowar M.K and Dewangan N.K, Parameter Estimation of Electrical Model of Heart by Modeling and Simulating Cardiovascular Variables, Int. J. Engg. Techsci, 2 (4), 2011, 296 – 301.

Ohlsson A, Nordlander R, Bennett T, Bitkover C, Kjellstr Bom, Lee B and Ryden L, Continuous ambulatory haemodynamic monitoring with an implantable system. The feasibility of a new technique, Eur. Heart J., 19, 1998, 174–184.

Poirier V.L, The LVAD, A case study, The Bridge, 27, 1997, 14–20.

Simaan M.A, Ferreira A, Chen S, Antaki J.F and Galati D.G, A Dynamical State space Representation and Performance Analysis of a Feedback controlled Rotary Left Ventricular Assist Device, IEEE Transactions on Control systems Technology, 17, 2009, 15-28.

Simaan M.A, Rotary Heart Assist Devices, Springer Handbook of Automation, Part H, 79, 2009, 1409-1422.

Stergiopulos N, Westerhoft B.E, Meister J.J and WesterhofS N, The Four Element Windkessel Model, 18th Annual International Conference of the IEEE Engineering in Medicine and Biology Society, Amsterdam, Physiological Modelling – Cardiovascular, 6 (2.5), 1996, 1715 – 1716.

Suga H and Sagawa K, Instantaneous pressure-volume relationships and their ratio in the excised, supported canine left ventricle, Circulatory Res., 35 (1), 1974, 117–126.